

Chromosome-level genome assembly and annotation of two lineages of the ant *Cataglyphis hispanica*: steppingstones towards genomic studies of hybridogenesis and thermal adaptation in desert ants

Hugo DARRAS^{1,2,a,*}, Natalia de Souza ARAUJO^{1,3,*}, Lyam BAUDRY^{4,6}, Nadège GUIGLIELMONI^{1,7}, Pedro LORITE⁵, Martial MARBOUTY⁶, Fernando RODRIGUEZ⁸, Irina ARKHIPOVA⁸, Romain KOSZUL⁶, Jean-François FLOT^{1,3}, Serge ARON¹

¹ Unit of Evolutionary Biology & Ecology, Université libre de Bruxelles (ULB), Brussels, Belgium

² Department of Ecology and Evolution, University of Lausanne, Lausanne, Switzerland

³ Interuniversity Institute of Bioinformatics in Brussels – (IB)² Brussels, Belgium

⁴ Centre for Integrative Genomics, University of Lausanne, Lausanne, Switzerland

⁵ Department of Biología Experimental, Universidad de Jaén, Jaén, Spain

⁶ Unité Régulation Spatiale des Génomes, CNRS, Institut Pasteur, Paris, France

⁷ Universität zu Köln, Köln, Germany

⁸ Marine Biological Laboratory, Woods Hole, Massachusetts, USA

^a corresponding author: Darras, H. hgdarras@gmail.com

* Authors contributed equally to this study

1 **ABSTRACT**

2 *Cataglyphis* are thermophilic ants that forage during the day when temperatures are highest and
3 sometimes close to their critical thermal limit. Several *Cataglyphis* species have evolved unusual
4 reproductive systems such as facultative queen parthenogenesis or social hybridogenesis, which
5 have not yet been investigated in detail at the molecular level. We generated high-quality genome
6 assemblies for two hybridogenetic lineages of the Iberian ant *Cataglyphis hispanica* using long-read
7 Nanopore sequencing and exploited chromosome conformation capture (3C) sequencing to
8 assemble contigs into 26 and 27 chromosomes, respectively. Males of one lineage were karyotyped
9 to confirm the number of chromosomes inferred from 3C data. We obtained transcriptomic data to
10 assist gene annotation and built custom repeat libraries for each of the two assemblies.
11 Comparative analyses with 19 other published ant genomes were also conducted. These new
12 genomic resources pave the way for exploring the genetic mechanisms underlying the remarkable
13 thermal adaptation and the molecular mechanisms associated with transitions between different
14 genetic systems characteristics of the ant genus *Cataglyphis*.

15

16 **KEYWORDS**

17 Social insects; *Cataglyphis*; Genome assembly; Genome annotation; karyotype; social
18 hybridogenesis

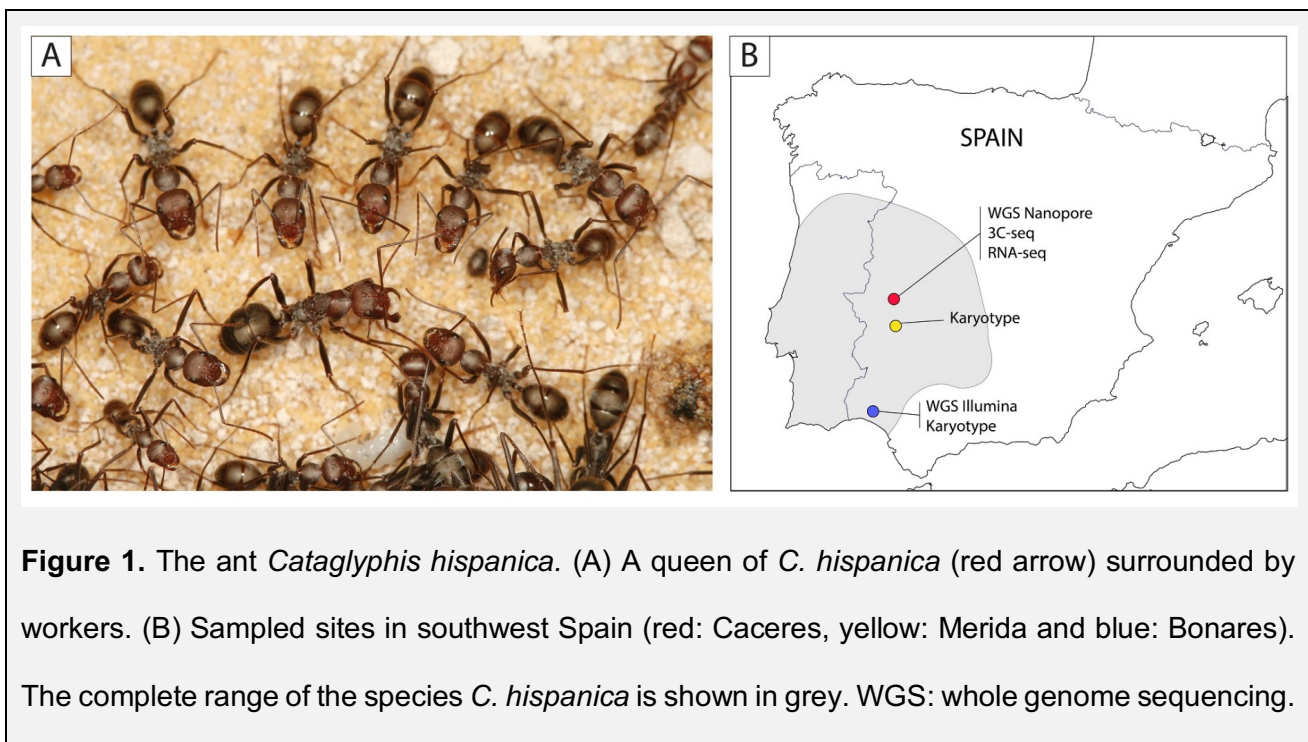
19 **BACKGROUND**

20 Ants of the genus *Cataglyphis* inhabit arid regions throughout the Old World, including inhospitable
21 deserts such as the Sahara (Lenoir et al. 1990; Boulay et al. 2017). Their foraging activities are
22 strictly diurnal, with most species being active during the hottest hours of the day (Wehner *et al.*,
23 1992; Cerda *et al.*, 1998). Some *Cataglyphis* species even forage at temperatures close to their
24 critical thermal limits (Cerda *et al.*, 1998). For instance, workers of the silver ant *Cataglyphis*
25 *bombycina* have been observed to forage when ground temperatures exceed 60°C (Wehner *et al.*,
26 1992), which provides a competitive advantage against lizard predators who avoid such harsh
27 conditions. The high thermal tolerance seen in *Cataglyphis* species relies on a range of behavioral,
28 morphological, physiological and molecular adaptations, such as exploitation of thermal refuges,
29 elongated legs, high speed of movement and intense recruitment of heat-shock chaperone proteins
30 (Gehring & Wehner 1995; Perez & Aron 2020; Pfeffer et al. 2019; Sommer & Wehner 2012; Willot
31 et al. 2017; Perez et al. 2021; Aron & Wehner 2021).

32 In addition to their impressive heat tolerance, *Cataglyphis* ants are prominent social insect
33 models because of their amazing diversity of reproductive traits: the number of queens per colony,
34 the mating frequencies, the dispersal strategies and the modes of production of different castes all
35 vary greatly among species (Aron, Mardulyn, and Leniaud 2016; Peeters and Aron 2017; Aron et
36 al. 2016). Unusual reproductive systems relying on conditional use of sex for the production of
37 different female castes have evolved repeatedly in different *Cataglyphis* groups. Under these
38 systems, non-reproductive workers are sexually produced, while reproductive queens are asexually
39 produced by thelytokous parthenogenesis – a strategy that allows queens to increase the
40 transmission rate of their genes to their reproductive female offspring while maintaining genetic
41 diversity in the worker force (Pearcy et al. 2004; Kuhn et al. 2020). Males arise from arrhenotokous
42 parthenogenesis, as is usually the case in Hymenoptera. In several species, the conditional use of
43 sex evolved into a unique reproductive system, named clonal social hybridogenesis, whereby male
44 and female sexuals are produced by parthenogenesis while workers are produced exclusively from
45 interbreeding between two sympatric, yet non-recombining genetic lineages (Leniaud et al. 2012;
46 Eyer et al. 2013; Kuhn et al. 2020).

47 The unique characteristics of *Cataglyphis* make this ant genus an interesting model to
48 investigate the genetic mechanisms underlying thermal adaptation and the evolution of alternative
49 reproductive strategies. To date, only one incomplete assembly of the genome of one species
50 (*Cataglyphis niger*) is available for genomic analyses (Yahav & Privman, 2019). To fill this gap, we
51 combined Oxford Nanopore long reads, Illumina short reads and chromosome conformation
52 capture (3C) sequencing (Lieberman-Aiden et al. 2009; Marie-Nelly et al. 2014; Flot, Marie-Nelly,
53 and Koszul 2015) to generate high-quality chromosome-scale genome assemblies of two lineages
54 of the Iberian ant *Cataglyphis hispanica* (Figure 1). We also annotated and compared the repeats
55 and gene sets of this species with those of other ant genera.

56
57



62

63 RESULTS AND DISCUSSION

64 Genome assembly

65 *Cataglyphis hispanica* inhabits the most arid habitats of the Iberian Peninsula. Two sympatric
66 hybridogenetic lineages (Chis1 and Chis2) co-occur as a complementary pair across the distribution
67 range of the species (Leniaud *et al.*, 2012; Darras *et al.*, 2014). Queens of each lineage mate with
68 males from the other lineage and produce non-reproductive workers by sexual reproduction. By

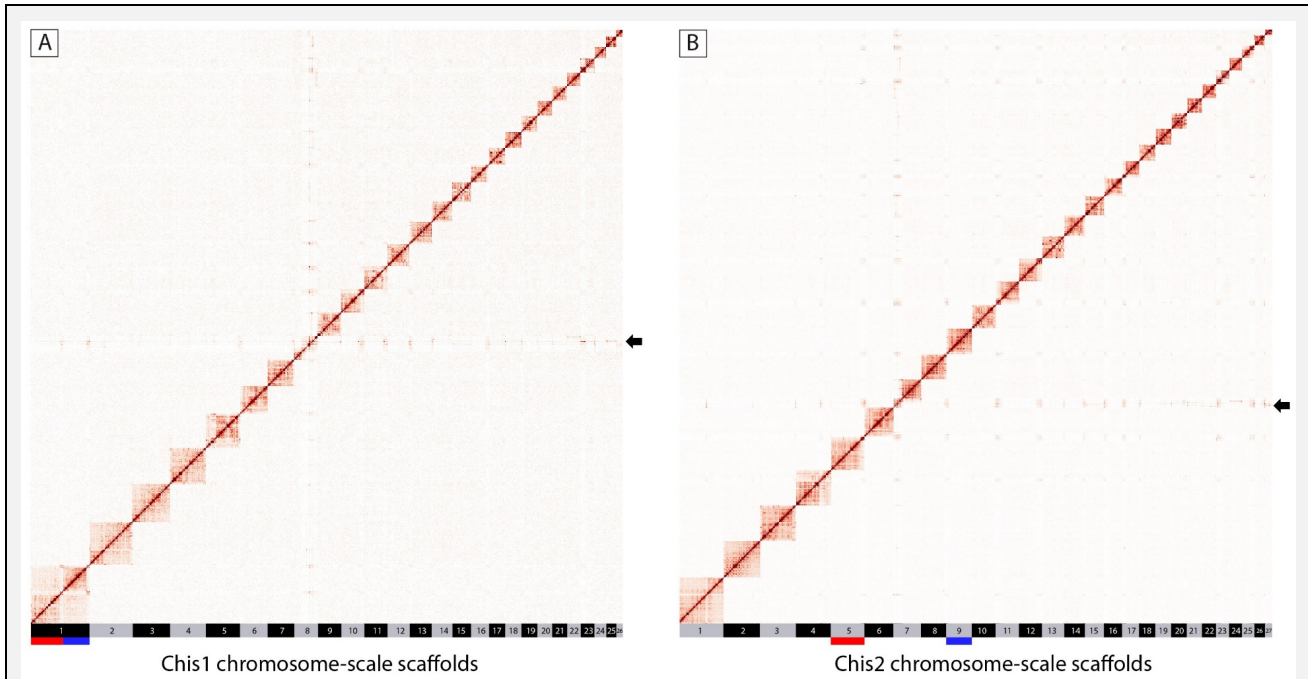
69 contrast, male and female reproductive individuals are produced clonally through arrhenotokous
70 and thelytokous parthenogenesis, respectively. As a result, all workers in the colonies are inter-
71 lineage hybrids, but the two reproductive lineages are maintained divergent.

72 For each of the Chis1 and Chis2 lineages, we generated respectively 5.7 and 5.1 Gbp of
73 Nanopore reads from a pool of sister clonal queens (for *de novo* long-read assemblies); 32.2 and
74 34.2 Gbp of PE 2 x 100 bp Illumina reads with insert sizes ranging from 170 bp to 800 bp from a
75 single male (for short read error correction/polishing); and 8.7 and 7.0 Gbp of 3C-seq PE 2 x 66 bp
76 (after demultiplexing) Illumina reads from a single queen (for scaffolding). The long-read assembler
77 Flye (Kolmogorov *et al.*, 2019) generated assemblies consisting of several hundreds of contigs (439
78 and 929, respectively). The contigs were scaffolded using the 3C data (Marie-Nelly *et al.*, 2014;
79 Baudry *et al.*, 2020): 99.7% of the Chis1 assembly was scaffolded into 26 chromosome-scale (> 2.4
80 Mb in length) scaffolds (Figure 2A), while 98.8 % of the Chis2 assembly was scaffolded into 27
81 chromosome-scale scaffolds (Figure 2B). These chromosome-scale scaffolds were numbered by
82 decreasing size. The remaining 0.3 – 1.2% unscaffolded sequences were all relatively small (<40
83 kb for Chis1, <120 kb for Chis2). The overall sizes of the two scaffolded assemblies were 203 Mb
84 and 209 Mb, respectively. Assembly completeness, as estimated by BUSCO scores (Manni *et al.*,
85 2021), was very high: among the 5,991 highly conserved single-copy genes of the Hymenoptera
86 odb10 database, 96.8% (Chis1) and 96.1% (Chis2) were complete in each assembly. In addition,
87 only 0.5-0.4% of the BUSCO genes appeared duplicated for both assemblies, suggesting that our
88 assemblies do not contain much uncollapsed haplotypes, if any. In line with these results, KAT
89 analyses based on the Illumina reads of each lineage showed a single peak of k-mer multiplicity,
90 which were almost all represented exactly once in the assemblies as expected for high-quality
91 genomes (Figure S1); k-mer completeness was estimated as 98.86% for Chis1 and 98.45% for
92 Chis2 (Mapleson *et al.*, 2016). For each assembly, a region with no large-scale synteny pattern
93 was assembled at the extremity of one scaffold (the first 5.4 Mb of scaffold #9 of Chis1 and the first
94 3.1 Mb of scaffold #7 of Chis2). Each of these regions consisted of a collection of small contigs
95 (mostly in the 2-10 Kb range) with 2 to 5 times higher average coverage compared to other genomic
96 regions. These problematic sequences exhibited microsynteny with the extremities of other large

97 scaffolds (Figure 2; Figure S2) suggesting that they correspond to repeat sequences that were
98 improperly assembled into fragmented contigs.

99

100



101

102 **Figure 2.** Assembly of the *Cataglyphis hispanica* Chis1 (A) and Chis2 (B) genomes into
103 chromosomes. Hi-C interaction map revealing the presence of 26 and 27 linkage groups. The color
104 scale represents the interaction frequencies. The positions of the rearranged chromosome are
105 indicated, and the arrows show the assembly artefact found in each genome (see main text). The
106 longest chromosome of Chis1 is split in two chromosomes in Chis2 (scaffolds 5 and 9, shown with
107 red and blue colors).

108

109 Comparison of the Chis1 and Chis2 assemblies revealed that 25 of the chromosome-scale
110 scaffolds had a one-to-one homolog in each of the two lineages. In addition, and by contrast, the
111 largest scaffold of Chis1 (#1) was split into two chromosome-scale scaffolds (# 5 and #10) in the
112 Chis2 assembly (Figure S2). The 3C contact maps of both lineages showed that these scaffolds
113 (Chis2 #5, #10 and Chis1 #1) correspond to well-individualized 3D features, thereby ruling out a
114 scaffolding error (Figure 2). These observations support that a chromosome centric (Robertsonian)
115 translocation took place in one of the two lineages studied. Centric fusions and fissions are the main

116 mechanisms of karyotype evolution in many animal groups, including ants (Lorite & Palomeque,
117 2010). Robertsonian translocations have been reported to promote speciation through the
118 suppression of genetic recombination in the vicinity of rearranged centromeric regions or the
119 reduction of fertility in karyotypic hybrids (Davisson & Akesson, 1993; Faria & Navarro, 2010). The
120 significance of this genomic rearrangement for the origin of social hybridogenesis in *Cataglyphis*
121 deserves further investigation. A different number of chromosomes among lineages could
122 potentially reduce the fertility of inter-lineage hybrids and may contribute to the long-term
123 maintenance of divergent lineages (Schwander, Keller, and Cahan 2007). Notably, two species
124 closely related to *C. hispanica* also reproduce by social hybridogenesis involving two
125 interdependent lineages (Eyer et al., 2013). We have previously speculated that this recurrent
126 genetic system may have evolved prior to the speciation of these three species. Under this scenario,
127 social hybridogenesis would be controlled by an ancient biallelic non-recombining region
128 maintained by chromosomal rearrangement(s), with two haplotypes accounting for the occurrence
129 of two genetic lineages in each species (Darras et al., 2014).

130 Intrachromosomal rearrangements between the lineages, consisting in large translocations and
131 inversions, were also observed for 6 of the 25 large orthologous scaffolds (Figure S2), but these
132 could not be confirmed independently with the current data.

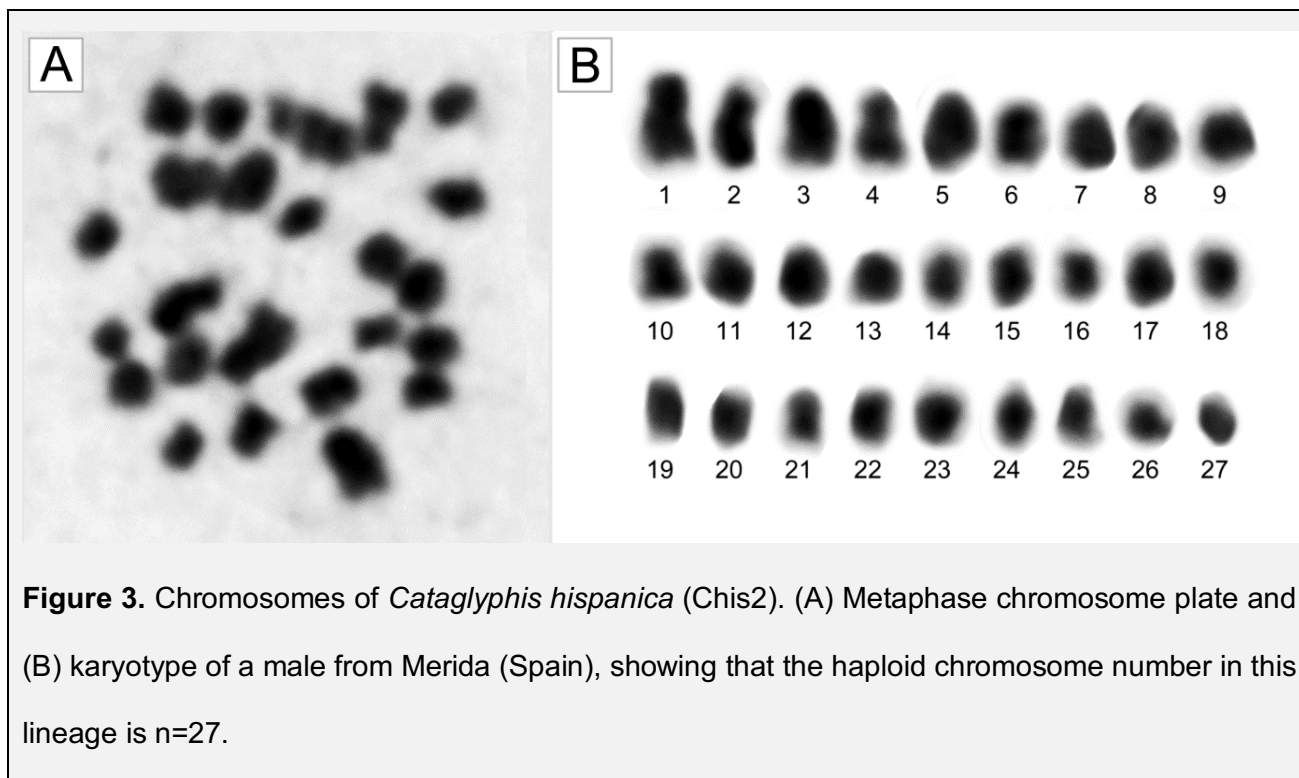
133

134 **Karyotyping**

135 To validate the number of chromosomes scaffolded, we inspected metaphase chromosome plates
136 from haploid males. In ants, as in other Hymenoptera, females are diploid ($2n$) whereas males are
137 haploid (n). Two males of the Chis2 lineage from two distant localities were analyzed (Figure S3A).
138 Both male karyotypes carried 27 chromosomes. The precise morphology of the chromosomes could
139 not be determined due to their small sizes (Figure 3). This number is within the range reported for
140 *Cataglyphis bicolor*, *Cataglyphis iberica* and *Cataglyphis setipes* species and other Formicine
141 species of the genera *Formica*, *Iberoformica* and *Polyergus* ($n= 26-27$) (Hauschteck-Jungen &
142 Jungen, 1983; Imai *et al.*, 1984; Lorite & Palomeque, 2010). These results confirm the 3C

143 scaffolding of the Chis2 genome into 27 chromosomes. No male of the Chis1 lineage could be
144 obtained for karyotyping.

145



146

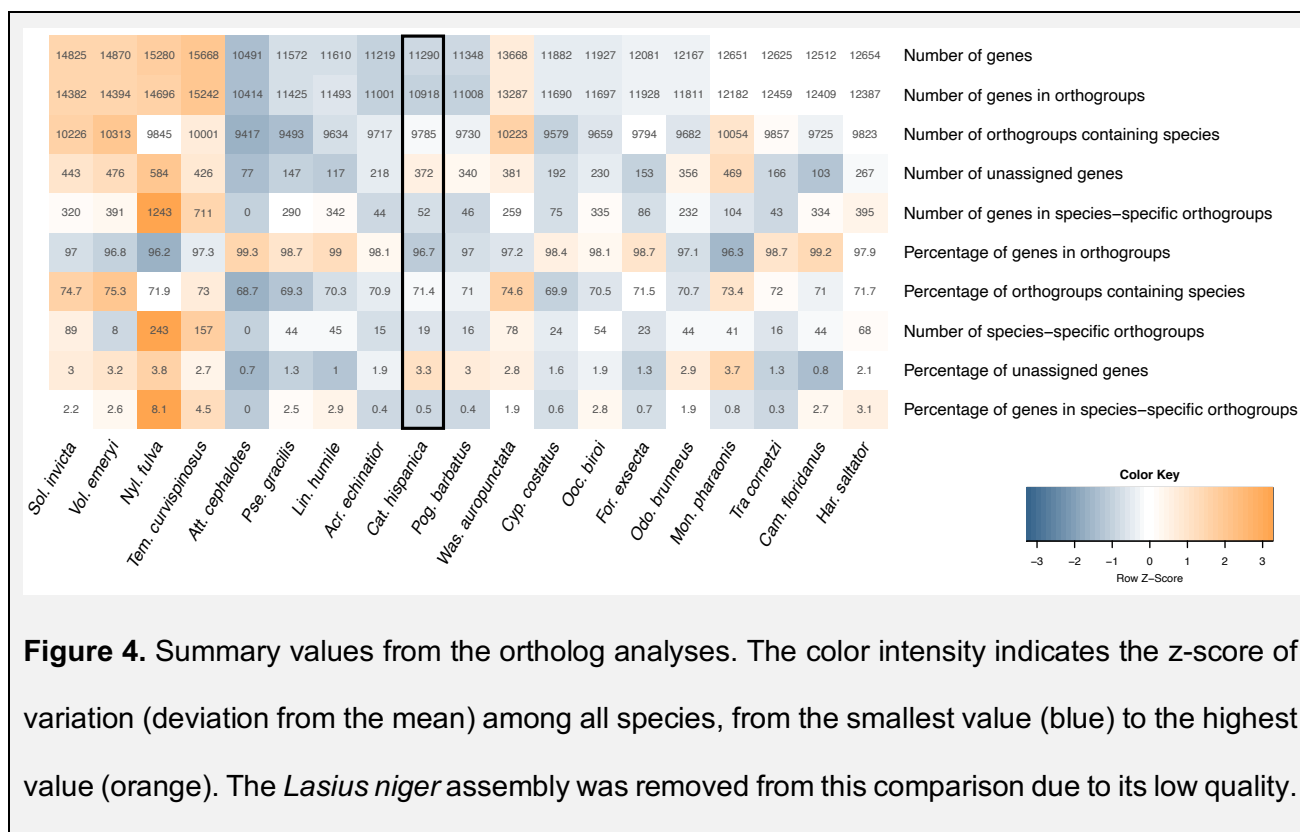
147 **Figure 3.** Chromosomes of *Cataglyphis hispanica* (Chis2). (A) Metaphase chromosome plate and
148 (B) karyotype of a male from Merida (Spain), showing that the haploid chromosome number in this
149 lineage is $n=27$.

150

151 Gene annotation

152 We annotated the genome of the Chis2 lineage. *Ab initio* gene prediction using AUGUSTUS and
153 homology-based predictions using GenomeThreader (Gremme *et al.*, 2005) identified 16,993 and
154 8,234 gene models, respectively. A total of 40,969 models (including isoforms) were also predicted
155 by the PASA/Transdecoder (Haas *et al.*, 2003) pipeline using direct evidence from 13 Gbp of
156 Illumina RNA-seq data. The three annotation sets were validated and combined into a single
157 annotation of 16,146 non-overlapping models using EvidenceModeler (Haas *et al.*, 2008). Among
158 these, 11,101 gene models showed significant similarity to at least one RefSeq ant protein and
159 10,543 had a functional eggNOG hit (Huerta-Cepas *et al.* 2017, 2019). After filtering out models
160 with no protein similarity and no known functional information, we obtained a final set of 11,290 high
161 quality gene models. This gene set is comparable in size to those annotated by the NCBI Eukaryotic
162 Genome Annotation Pipeline for other ant genomes (range: 10,491-15,668; N= 18 different RefSeq
163 ant genera; Table S1). We compared the gene set of *C. hispanica* (Chis2) with 19 published ant

164 annotations. Out of the 258,587 protein-coding genes analyzed using OrthoFinder (Emms & Kelly,
 165 2019), 96.82% (250,353) were placed in 13,698 orthogroups. Of these, 1,407 were species-specific
 166 and 6,199 were found in all species including 3,365 single-copy genes. The orthogroup profile of *C.*
 167 *hispanica* was overall comparable to that of other ants (Figure 4). However, our annotation had one
 168 of the smallest number of genes placed in orthogroups (10,918), and one of the largest proportions
 169 of unassigned genes (3.3%).
 170

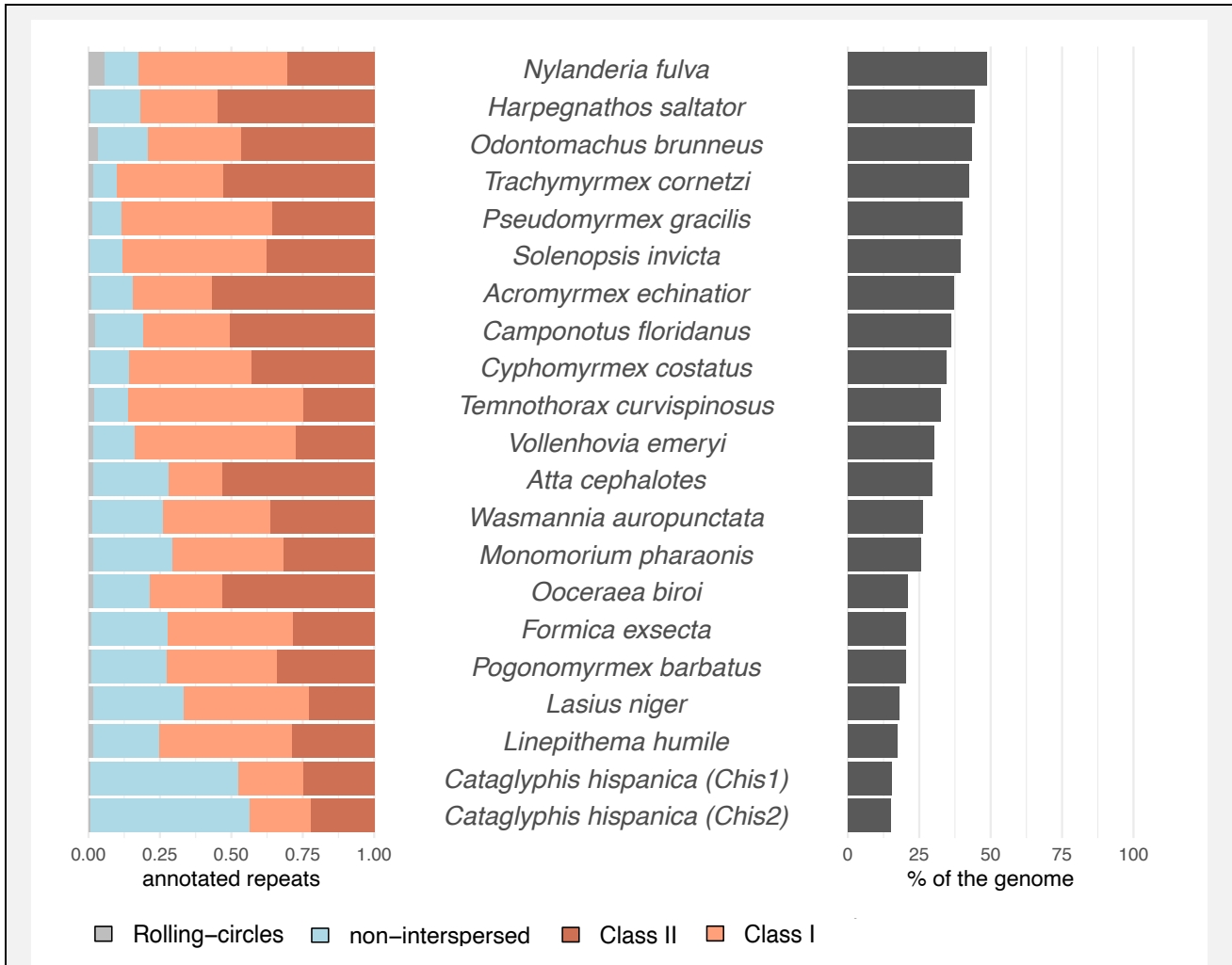


171
 172 **Figure 4.** Summary values from the ortholog analyses. The color intensity indicates the z-score of
 173 variation (deviation from the mean) among all species, from the smallest value (blue) to the highest
 174 value (orange). The *Lasius niger* assembly was removed from this comparison due to its low quality.
 175

176 Repeat annotation

177 We built custom repeat libraries for each of the two assemblies of *C. hispanica* and for 19 published
 178 ant genomes (Table S1). The Chis1 and Chis2 assemblies contained 1,708 and 1,673 different
 179 repetitive elements, which accounted for 15.43% (31,851,170 bp) and 15.1% (31,512,815 bp) of
 180 their assembly sizes, respectively (Figure 5). A large proportion of these corresponded to
 181 unclassified interspersed repeats (6.7% / 6.78% of the genomes; Figure S4). The two genomes
 182 also contained 2.0% / 1.8% of Class I (retroelements), and 2.18% / 1.85% of Class II elements
 183 (DNA transposons). In total, 56 different families of repetitive elements were annotated in *C.*

184 *hispanica*. LTR/Gypsy were the most frequent transposable elements of Class I in the genomes
 185 (0.53% / 0.82%), while large Polintons / Mavericks were the most abundant Class II transposable
 186 elements (0.98% / 0.67%).



187
 188 **Figure 5.** Summary of the repetitive elements' categories annotated in 20 different ant species using
 189 our custom pipeline. The ratios of the major categories of repetitive elements identified in each
 190 species is shown on the left. The total proportion of repetitive elements found in each genome is
 191 shown on the right.

192
 193 Across published ant assemblies, the total proportion of transposable elements appeared quite
 194 variable (range: 17.27 – 48.47%; N= 19 ant species; Figure 5; Table S2). The *C. hispanica*
 195 assemblies had a smaller proportion of repetitive elements (15.1% - 15.43%) than any of these
 196 assemblies. This difference in repeat content was slightly smaller when compared to the assembly

197 of *Formica exsecta* (18.53 %), the closest species available for comparison. The relatively low
198 proportion of transposable elements observed in the genomes of *C. hispanica* may be due to the
199 fact that it was assembled primarily from noisy nanopore long-reads, possibly leading to a collapse
200 of repeated regions. Alternatively, *C. hispanica* may resist the invasion and proliferation of
201 transposable elements more efficiently than other species. Whether its unusual reproductive
202 system, combining both diploid and haploid parthenogenesis for queen and male production, could
203 help keep transposable elements at bay deserves further exploration.

204

205 **Lineage divergence estimation**

206 To estimate divergence between the two genomes sequenced, we analyzed polymorphism at four-
207 fold-degenerate sites, which are expected to be neutrally evolving (every mutation at a four-fold site
208 is synonymous). Our annotation of the Chis2 genome contained 2,620,448 four-fold-degenerate
209 sites. Among these, 13,048 had a different allele in the Chis1 and Chis2 males used to obtain
210 haploid genome consensus. Assuming no recombination and a typical insect mutation rate of
211 approximately 3×10^{-9} mutations per neutral site per haploid genome per generation (Keightley *et*
212 *al.*, 2014, 2015; Yang *et al.*, 2015; Liu *et al.*, 2017; Oppold & Pfenninger, 2017), this proportion of
213 mutated four-fold-degenerate sites translated into an average divergence time of about 830,000
214 generations between the alleles of the two males sequenced (Obbard *et al.*, 2012). Hence, the two
215 genome sequenced may have diverged almost 1 million years ago (assuming one generation per
216 year) - a divergence time similar to what observed between closely related species of fire ants
217 (Cohen & Privman, 2019). The origin of the hybridogenetic lineages themselves could be much
218 younger if these emerged in two divergent populations or share ancestral polymorphism (Darras *et*
219 *al.* 2019).

220

221 **CONCLUSIONS**

222 We generated high-quality chromosome level genome assemblies of the two lineages of the
223 hybridogenetic ant *C. hispanica*, a representative species of the thermophilic ant genus *Cataglyphis*.
224 Using chromosome conformation capture, we identified a Robertsonian translocation between the

225 two lineages, resulting in 26 and 27 chromosomes in Chis1 and Chis 2 lineages, respectively.
226 Whether this rearrangement played a role in the origin and maintenance of social hybridogenesis
227 in *C. hispanica* and across other *Cataglyphis* species deserves further investigation (Darras *et al.*,
228 2014).

229

230

231 **METHODS**

232 **Biological samples**

233 Permits were obtained to collect colonies of *Cataglyphis hispanica* in three Spanish locations
234 (Bonares, Caceres and Merida; Figure 1B). Male samples from Bonares were used for Illumina
235 DNA sequencing. Shortly after sampling, the Bonares population was wiped out by human activities.
236 Consequently, samples from another locality (Caceres) were used for subsequent Nanopore
237 sequencing, 3C-seq and RNA-seq. Male pupae from two distant localities (Bonares and Merida)
238 were used for karyotyping. Twelve diagnostic microsatellite loci were genotyped to assess the
239 lineage membership of each queen and male prior to sequencing and karyotyping (Darras *et al.*,
240 2014).

241

242 **DNA and RNA-Sequencing**

243 Genomic resources were generated for both the Chis1 and the Chis2 lineages. High-molecular-
244 weight DNA was extracted from pure lineage queen and male individuals using QIAGEN Genomic-
245 tips. For each lineage, two queen clones originating from the same nest were used for Nanopore
246 sequencing. Queens of *C. hispanica* are produced through automictic parthenogenesis with central
247 fusion which results into diploid individuals that are highly homozygous (Pearcy *et al.*, 2011; Darras
248 *et al.*, 2014) and thus suitable for genome assembly. Nanopore libraries were prepared using rapid
249 sequencing kits (SQK-RAD001 and SQK-RAD004). The resulting long read libraries were
250 sequenced on MIN106 flow cells and basecalled using Albacore v2.1.10. For each lineage, three
251 Illumina libraries were generated from whole-genome amplified DNA extracted from a single male

252 with mean insert sizes of 170 bp, 500 bp and 800 bp, and sequenced with a HiSeq2000 (paired-
253 end 2 x 100 bp mode).

254 3C-seq libraries were prepared according to the protocol described in (Marie-Nelly *et al.*, 2014).
255 Briefly, queens from both lineages had their gut removed and were immediately suspended in 30
256 mL of formaldehyde solution (Sigma Aldrich; 3% final concentration in 1X tris-EDTA buffer). After
257 one hour of incubation, quenching of the remaining formaldehyde was done by adding 10 mL of
258 glycine (0.25 M final concentration) to the mix for during 20 min. The cross-linked tissues were
259 pelleted and stored at -80°C until further use. The 3C-seq libraries were prepared using the *DpnII*
260 enzyme and sequenced using an Illumina NextSeq 500 apparatus (paired-end 2x75 bp; first ten
261 bases corresponding to custom-made tags). 3C-seq libraries are similar to Hi-C libraries except that
262 they contain a higher percentage of paired-end reads due to the lack of an enrichment step (Flot,
263 Marie-Nelly, and Koszul 2015).

264 To help annotate the genomes, three normalized RNA-seq cDNA Illumina libraries were obtained:
265 one from an adult Chis1 queen, one from a Chis2 queen and one from a pool of brood of different
266 stages and adult workers originating from colonies of the two lineages (HiSeq2000, paired-end 2 x
267 100 bp mode).

268

269 **Genomes assembly**

270 The genome of each hybridogenetic lineage was assembled independently. Nanopore data were
271 assembled using Flye v2.7 with four iterations of polishing using long reads (Kolmogorov *et al.*,
272 2019). Raw Illumina reads were trimmed for quality and adapters were removed using Trimmomatic
273 v0.32 with options ILLUMINACLIP:TruSeq3-PE-2.fa:2:30:10 LEADING:3 TRAILING:3
274 SLIDINGWINDOW:4:15 MINLEN:36 (Bolger *et al.*, 2014). The trimmed reads were then aligned to
275 the long-read assemblies using BWA-MEM v0.7.15 (Li & Durbin, 2009). SNPs and indels with at
276 least three supporting observations were called using freebayes v1.2 (Garrison & Marth, 2012), and
277 error-corrected consensus sequences were obtained using BCFtools v1.4 (Li *et al.*, 2009).

278 To obtain chromosome-scale assemblies, we scaffolded the polished contigs with the 3C reads
279 using instaGRAAL, a MCMC, proximity-ligation based scaffolder (Marie-Nelly *et al.*, 2014; Baudry

280 *et al.*, 2020). The 3C reads were trimmed using cutadapt (Martin, 2011) and subsequently
281 processed using hicstuff (<https://zenodo.org/record/4722873>) with the following parameters –
282 *aligner bowtie2 –iterative –enzyme DpnII*. The instaGRAAL scaffolder was run on the pre-processed
283 data for 100 cycles (parameters: level 4, with options *--coverage-std 1 –level 4 –cycles 100*) (Baudry
284 *et al.*, 2020) and final scaffolds were obtained using the instaGRAAL *-polish* script, with all corrective
285 procedures at once (only one parameter: *-m polish*). Briefly, instaGRAAL explores the chromosome
286 structures by testing the relative positions and/or orientations of DNA segments (or bins) according
287 to the contacts expected given a simple three-parameter power-law model. These modifications
288 take the form of a fixed set of operations (swapping, flipping, inserting, merging, etc.) of bins
289 corresponding to $3^4 = 81$ *DpnII* restriction fragments. The likelihood of the model is then maximized
290 by sampling the parameters using a MCMC approach (Marie-Nelly *et al.*, 2014). After 100 iterations
291 (i.e., a likely position for each bin is tested 100 times), the genome structure converges towards a
292 relatively stable structure that does not evolve anymore when more iterations are added, resulting
293 in chromosome-level scaffolds. The algorithm is probabilistic and ignores initially part of the intrinsic
294 structure of the original contigs in order to sample a larger range of genome space (Baudry *et al.*,
295 2020). Therefore, some trustworthy information contained in the initial polished assembly can be
296 lost, or modified, along the way. The final correction step of instaGRAAL consists in reintegrating
297 this lost information into the final assembly, to correct for instance local untrustworthy tiny inversions
298 of individual bins within a contig. The contact maps of the scaffolded assemblies were built using
299 hicstuff. Gaps created during the scaffolding process were closed using Nanopore data with four
300 iterations of TGS-GapCloser (Xu *et al.*, 2019) and new polished consensus sequences were
301 obtained using BCFtools (see method above). Completeness of the assemblies were assessed at
302 each step using BUSCO v5.2.2 with the Hymenoptera odb10 lineage (Simão *et al.*, 2015;
303 Waterhouse *et al.*, 2017). We also ran KAT v2.4.1 to compare the k-mer frequencies of Illumina
304 reads to final assemblies (Mapleson *et al.*, 2016). To investigate differences in chromosomal
305 arrangement among lineages, the two genome assemblies were aligned with minimap2 v2.17
306 (exact preset: *-x asm5*) and alignments were visualized using dot plots obtained with D-GENIES
307 (Cabanettes & Klopp, 2018).

308

309 **Karyotyping**

310 To validate the number of chromosomes inferred from 3C contact information, chromosome
311 preparations were made from brains of male larvae following the protocol described by (Lorite *et*
312 *al.*, 1996), with some modifications. Briefly, larvae at the last instar stage were dissected and their
313 cerebral ganglia were transferred to microplate wells with 0.05% colchicine in distilled water. After
314 30 min, samples were transferred to a fixative solution (acetic acid:ethanol, 3:1) and incubated for
315 45 min. Ganglia cells were disaggregated in a drop of 50% acetic acid on a clean slide, new fixative
316 solution was added and the slides were dried at 60°C. Chromosome preparations were stained with
317 10% Giemsa in phosphate buffer (pH 7). Microscopy images were captured with a CCD camera
318 (Olympus DP70) coupled to a microscope (Olympus BX51) and were processed using Adobe
319 Photoshop.

320

321 **Gene annotation**

322 We used the *Chis2* chromosome-level assembly for gene annotation. A repeat library was
323 constructed using the REPET package v2.5 (Quesneville *et al.*, 2005; Flutre *et al.*, 2011). The
324 repeat library was cleaned up manually to remove bacterial genes, mitochondrial genes and genes
325 with hits to the gene set of the ant *Cardiocondyla obscurior* (v1.4) which had been purged of
326 transposable elements (Schrader *et al.*, 2014). The fraction of the genome classified by
327 RepeatClassifier as "Unknown" was reduced from 2.2% to 0.9% as a result of this procedure.
328 Repeats were soft-masked using RepeatMasker v4.0.7 (Smit and Hubley,
329 <http://www.repeatmasker.org>) prior to *de novo* gene prediction.

330 Gene models were inferred from RNA-seq, homology data and *ab initio* predictions. The three
331 RNA-seq libraries were aligned to the *Chis2* genome using STAR v2.6.0 (Dobin *et al.*, 2013) with
332 the multi-sample 2-pass mapping strategy. Transcripts were then assembled using Trinity v2.10.0
333 (Grabherr *et al.*, 2011; Haas *et al.*, 2013)(options --genome_guided_max_intron 100000 --
334 jaccard_clip) and combined into gene models using PASA (Haas *et al.*, 2003). Ant proteomes
335 annotated using the NCBI Eukaryotic Genome Annotation pipeline (RefSeq, taxid:36668) were

336 aligned to the genome using GenomeThreader v1.5.10 (Gremme *et al.*, 2005) in order to predict
337 gene structures. AUGUSTUS *ab initio* predictions were generated using BRAKER v2.1.02 (Hoff *et*
338 *al.*, 2016, 2019) based on hints from RNA-seq data and GenomeThreader protein alignments (--
339 etpmode). BRAKER was first run with preliminary AUGUSTUS parameters trained by running
340 BUSCO v3.0.2 on the genome assembly (--long option; Hymenoptera odb9 database). To refine
341 the training of AUGUSTUS, the most accurate gene models inferred by BRAKER were then
342 identified using GeneValidator (Drăgan *et al.*, 2016) with RefSeq ant proteomes as references and
343 an arbitrary quality threshold of Q89. To avoid biases, predicted proteins with more than 70%
344 sequence identity to another protein in the set were removed from the selected gene models using
345 the aa2nonred.pl script provided with BRAKER. The resulting gene models were used to train
346 AUGUSTUS again, and BRAKER was run with the new parameter set. *Ab initio*, RNA-seq-based
347 and homology-based gene predictions were combined into a single gene set using
348 EVIDENCEModeler v1.1.1 (Haas *et al.*, 2008) with the following weight settings: PASA alignments:
349 10; GenomeThreader alignments: 3, Augustus predictions: 1, PASA/Transdecoder predictions: 1,
350 GenomeThreader predictions: 1. Functional information was obtained from eggNOG-mapper v2
351 (Huerta-Cepas *et al.* 2017, 2019) with the options "taxonomic scope adjusted per query" and
352 "annotations transferred from any ortholog". Protein sequences with similarity to RefSeq ant
353 proteins (as of July 2019) were identified using blastp and an E-value threshold of 10^{-5} . Annotations
354 with no known functional information and no hits to any RefSeq ant proteins were filtered out.

355

356 **Comparative analyses**

357 To identify orthologous and taxonomically restricted genes (or orphan genes), we compared the
358 proteomes of *C. hispanica*, of 18 ants annotated by the NCBI Eukaryotic Genome Annotation
359 Pipeline (Table S1) and of *Lasius niger* (Konorov *et al.*, 2017) using OrthoFinder v2.3.12 (Emms &
360 Kelly, 2019) with its standard DEndroBLAST workflow. We used the feature annotation tables from
361 RefSeq annotations to select the longest isoform of each gene annotated by NCBI prior to analysis.
362 The published genome of *L. niger* is highly incomplete (no more than 65% of the 4,415 highly
363 conserved single-copy genes of BUSCO's Hymenoptera odb9 database are found in this

364 assembly). Consequently, it was only used to guide phylogenetic analyses due to its relative
365 proximity with *Cataglyphis*. A preliminary catalog of single-copy orthologs was obtained from a first
366 run of OrthoFinder. Single-copy sequences were aligned with Mafft v7.310 (Katoch & Standley, 2013)
367 and the alignments were trimmed with trimAL v1.4.1 (options "-gt 0.8 -st 0.001"; (Capella-Gutiérrez
368 *et al.*, 2009). The concatenated alignments were then passed to IQ-TREE v1.7.17 (Nguyen *et al.*
369 2015) "-m LG+R4"; (Nguyen *et al.*, 2015) to infer a species tree. The tree was converted to an
370 ultrametric topology with the r8s program with options "mrca root Obir Hsal; fixage taxon=root
371 age=150; divtime method=LF algorithm=TN" (Sanderson, 2003). The resulting species tree was
372 used for a second, more precise run of OrthoFinder.

373

374 **Repeat annotation**

375 To compare the frequency of repetitive elements found in the genome of *C. hispanica* to the
376 frequencies found in the genomes of other ant species available (Table S4), we constructed
377 optimized repeat libraries for each species using a custom pipeline
378 (https://github.com/nat2bee/repetitive_elements_pipeline). Shortly, repeat libraries were built with
379 RepeatModeler v1.0.11 (<http://www.repeatmasker.org/RepeatModeler/>), TransposonPSI
380 (<http://transposonpsi.sourceforge.net/>) and LTRharvest from GenomeTools v1.6.1 (Ellinghaus *et al.*, 2008). For each species, the different libraries were merged into a non-redundant library (<80%
381 identity) using USEARCH v11.0.667 (Edgar, 2010). Library annotations were obtained with
382 RepeatClassifier. Each custom library was concatenated with the Dfam v3.1 Hymenoptera library
383 of RepeatMasker v4.1.0 and used to annotate repeats in the genome of the corresponding species
384 using RepeatMasker. Summary statistics of the annotated repeats was obtained with
385 RepeatMasker_stats.py (https://github.com/nat2bee/repetitive_elements_pipeline).

387

388 **Lineage divergence estimation**

389 To estimate the divergences of the two lineages of *C. hispanica*, we investigated the polymorphism
390 at 4-fold-degenerate sites, which we assumed to be neutrally evolving. The Illumina read of the
391 Chis1 lineage were mapped onto the Chis2 reference genome and single-nucleotide variants were

392 called using MapCaller v0.9.9.41 (Lin and Hsu 2019). The resulting vcf file was filtered to keep only
393 single-nucleotide variants with two alleles and a 'PASS' quality filter. To determine the proportion of
394 4-fold sites that were polymorphic among our male samples of the two lineages, the positions of 4-
395 fold sites in coding sequences of our annotation were identified using a custom script (T. Sackton,
396 github.com/tsackton/linked-selection.git).

397

398

399 **DECLARATIONS**

400 **Data Availability**

401 All the raw sequencing data and genome assemblies generated during this study have been
402 deposited at NCBI (Accession numbers: SRR17481978 - SRR17481992). The genomes of *C.*
403 *hispanica* were deposited in NCBI (Accession numbers: JAJUXC000000000 and
404 JAJUXE000000000). Supplementary figures, tables, gene annotations, TEs repeat libraries and
405 reports can be accessed at figshare (<https://doi.org/10.6084/m9.figshare.17964695>).

406

407 **Funding**

408 NSA and SA are supported by the Belgian Fonds National pour la Recherche Scientifique (FRS-
409 FNRS). NG was supported by the Horizon 2020 research and innovation program of the European
410 Union under the Marie Skłodowska-Curie grant agreement No. 764840 (ITN IGNITE, www.itn-ignite.eu) to JFF. This project was funded by the FRS-FNRS Grants # J.0151.16 and T.0140.18 (to
411 SA). HD received financial support from the Jean-Marie Delwart Foundation. Computational re-
412 sources were provided by the Consortium des Équipements de Calcul Intensif (CÉCI), funded by
413 the Belgian Fund for Scientific Research-FNRS (F.R.S.-FNRS; grant No. 2.5020.11).

415

416 **Authors' Contributions**

417 HD collected the ants, prepared DNA/RNA, assembled and annotated the genome. NSA performed
418 TE analyses and genomic comparisons. Both HD and NSA prepared first manuscript draft. PL

419 performed karyotyping. LB optimized 3C scaffolding parameters. NG performed 3C scaffolding. MM
420 prepared the 3C libraries. FR constructed the TE library. IA supervised the construction of the TE
421 library. RK supervised 3C library generation and scaffolding. JFF supervised genome assembly.
422 SA collected the ants, designed and supervised the study. All authors read and approved the final
423 manuscript.

424

425 **Competing Interests**

426 The authors declare that they have no competing interests.

427

428 **Acknowledgments**

429 We thank A. Cohanim and E. Privman for their advices on early genome assemblies and Qiaowei
430 M. Pan for her comments on the manuscript.

431

432

433 **REFERENCES**

- 434 Aron, Serge, Pascale Lybaert, Claire Baudoux, Morgane Vandervelden, and Denis Fournier. 2016.
435 "Sperm Production Characteristics Vary with Level of Sperm Competition in *Cataglyphis*
436 *Desert Ants*." *Functional Ecology* 30 (4): 614–24.
- 437 Aron, Serge, Patrick Mardulyn, and Laurianne Leniaud. 2016. "Evolution of Reproductive Traits in
438 *Cataglyphis* Desert Ants: Mating Frequency, Queen Number, and Thelytoky." *Behavioral*
439 *Ecology and Sociobiology* 70 (8): 1367–79.
- 440 Aron, Serge, and Rüdiger Wehner. 2021. "Cataglyphis." In *Encyclopedia of Social Insects*, 217–23.
441 Cham: Springer International Publishing.
- 442 Baudry, Lyam, Nadège Guiglielmoni, Hervé Marie-Nelly, Alexandre Cormier, Martial Marbouty,
443 Komlan Avia, Yann Loe Mie, et al. 2020. "InstaGRAAL: Chromosome-Level Quality
444 Scaffolding of Genomes Using a Proximity Ligation-Based Scaffold." *Genome Biology* 21
445 (1): 148.

- 446 Bolger, Anthony M., Marc Lohse, and Bjoern Usadel. 2014. "Trimmomatic: A Flexible Trimmer for
447 Illumina Sequence Data." *Bioinformatics* 30 (15): 2114–20.
- 448 Boulay, Raphaël, Serge Aron, Xim Cerdá, Claudie Doums, Paul Graham, Abraham Hefetz, and
449 Thibaud Monnin. 2017. "Social Life in Arid Environments: The Case Study of *Cataglyphis*
450 *Ants*." *Annual Review of Entomology* 62 (January): 305–21.
- 451 Cabanettes, Floréal, and Christophe Klopp. 2018. "D-GENIES: Dot Plot Large Genomes in an
452 Interactive, Efficient and Simple Way." *PeerJ* 6 (June): e4958.
- 453 Capella-Gutiérrez, Salvador, José M. Silla-Martínez, and Toni Gabaldón. 2009. "TrimAl: A Tool for
454 Automated Alignment Trimming in Large-Scale Phylogenetic Analyses." *Bioinformatics* 25
455 (15): 1972–73.
- 456 Cerda, X., J. Retana, and S. Cros. 1998. "Critical Thermal Limits in Mediterranean Ant Species:
457 Trade-off between Mortality Risk and Foraging Performance." *Functional Ecology* 12 (1):
458 45–55.
- 459 Cohen, Pnina, and Eyal Privman. 2019. "Speciation and Hybridization in Invasive Fire Ants." *BMC*
460 *Evolutionary Biology* 19 (1): 111.
- 461 Darras, Hugo, Alexandre Kuhn, and Serge Aron. 2019. "Evolution of Hybridogenetic Lineages in
462 *Cataglyphis* Ants." *Molecular Ecology* 28 (12): 3073–88.
- 463 Darras, Hugo, Laurianne Leniaud, and Serge Aron. 2014. "Large-Scale Distribution of
464 Hybridogenetic Lineages in a Spanish Desert Ant." *Proceedings. Biological Sciences / The*
465 *Royal Society* 281 (1774): 20132396.
- 466 Davisson, M. T., and E. C. Akeson. 1993. "Recombination Suppression by Heterozygous
467 Robertsonian Chromosomes in the Mouse." *Genetics* 133 (3): 649–67.
- 468 Dobin, Alexander, Carrie A. Davis, Felix Schlesinger, Jorg Drenkow, Chris Zaleski, Sonali Jha,
469 Philippe Batut, Mark Chaisson, and Thomas R. Gingeras. 2013. "STAR: Ultrafast Universal
470 RNA-Seq Aligner." *Bioinformatics* 29 (1): 15–21.

- 471 Drăgan, Monica-Andreea, Ismail Moghul, Anurag Priyam, Claudio Bustos, and Yannick Wurm.
472 2016. "GeneValidator: Identify Problems with Protein-Coding Gene Predictions."
473 *Bioinformatics* 32 (10): 1559–61.
- 474 Edgar, Robert C. 2010. "Search and Clustering Orders of Magnitude Faster than BLAST."
475 *Bioinformatics* 26 (19): 2460–61.
- 476 Ellinghaus, David, Stefan Kurtz, and Ute Willhoeft. 2008. "LTRharvest , an Efficient and Flexible
477 Software for de Novo Detection of LTR Retrotransposons." *BMC Bioinformatics* 9 (1): 1–14.
- 478 Emms, David M., and Steven Kelly. 2019. "OrthoFinder: Phylogenetic Orthology Inference for
479 Comparative Genomics." *Genome Biology* 20 (1): 238.
- 480 Eyer, P. A., L. Leniaud, H. Darras, and S. Aron. 2013. "Hybridogenesis through Thelytokous
481 Parthenogenesis in Two *Cataglyphis* Desert Ants." *Molecular Ecology* 22 (4): 947–55.
- 482 Faria, Rui, and Arcadi Navarro. 2010. "Chromosomal Speciation Revisited: Rearranging Theory with
483 Pieces of Evidence." *Trends in Ecology & Evolution* 25 (11): 660–69.
- 484 Flot, Jean-François, Hervé Marie-Nelly, and Romain Koszul. 2015. "Contact Genomics: Scaffolding
485 and Phasing (Meta)Genomes Using Chromosome 3D Physical Signatures." *FEBS Letters*
486 589 (20 Pt A): 2966–74.
- 487 Flutre, Timothée, Elodie Duprat, Catherine Feuillet, and Hadi Quesneville. 2011. "Considering
488 Transposable Element Diversification in de Novo Annotation Approaches." *PloS One* 6 (1):
489 e16526.
- 490 Garrison, Erik, and Gabor Marth. 2012. "Haplotype-Based Variant Detection from Short-Read
491 Sequencing." *ArXiv [q-Bio.GN]*. arXiv. <http://arxiv.org/abs/1207.3907>.
- 492 Gehring, W. J., and R. Wehner. 1995. "Heat Shock Protein Synthesis and Thermotolerance in
493 *Cataglyphis*, an Ant from the Sahara Desert." *Proceedings of the National Academy of*
494 *Sciences of the United States of America* 92 (7): 2994–98.
- 495 Grabherr, Manfred G., Brian J. Haas, Moran Yassour, Joshua Z. Levin, Dawn A. Thompson, Ido
496 Amit, Xian Adiconis, et al. 2011. "Full-Length Transcriptome Assembly from RNA-Seq Data
497 without a Reference Genome." *Nature Biotechnology*. <https://doi.org/10.1038/nbt.1883>.

- 498 Gremme, Gordon, Volker Brendel, Michael E. Sparks, and Stefan Kurtz. 2005. "Engineering a
499 Software Tool for Gene Structure Prediction in Higher Organisms." *Information and Software
500 Technology* 47 (15): 965–78.
- 501 Haas, Brian J., Arthur L. Delcher, Stephen M. Mount, Jennifer R. Wortman, Roger K. Smith Jr, Linda
502 I. Hannick, Rama Maiti, et al. 2003. "Improving the Arabidopsis Genome Annotation Using
503 Maximal Transcript Alignment Assemblies." *Nucleic Acids Research* 31 (19): 5654–66.
- 504 Haas, Brian J., Alexie Papanicolaou, Moran Yassour, Manfred Grabherr, Philip D. Blood, Joshua
505 Bowden, Matthew Brian Couger, et al. 2013. "De Novo Transcript Sequence Reconstruction
506 from RNA-Seq Using the Trinity Platform for Reference Generation and Analysis." *Nature
507 Protocols* 8 (8): 1494–1512.
- 508 Haas, Brian J., Steven L. Salzberg, Wei Zhu, Mihaela Pertea, Jonathan E. Allen, Joshua Orvis,
509 Owen White, C. Robin Buell, and Jennifer R. Wortman. 2008. "Automated Eukaryotic Gene
510 Structure Annotation Using EVIDENCEModeler and the Program to Assemble Spliced
511 Alignments." *Genome Biology* 9 (1): R7.
- 512 Hauschteck-Jungen, E., and H. Jungen. 1983. "Ant Chromosomes." *Insectes Sociaux* 30 (2): 149–
513 64.
- 514 Hoff, Katharina J., Simone Lange, Alexandre Lomsadze, Mark Borodovsky, and Mario Stanke.
515 2016. "BRAKER1: Unsupervised RNA-Seq-Based Genome Annotation with GeneMark-ET
516 and AUGUSTUS: Table 1." *Bioinformatics*. <https://doi.org/10.1093/bioinformatics/btv661>.
- 517 Hoff, Katharina J., Alexandre Lomsadze, Mark Borodovsky, and Mario Stanke. 2019. "Whole-
518 Genome Annotation with BRAKER." *Methods in Molecular Biology*.
519 https://doi.org/10.1007/978-1-4939-9173-0_5.
- 520 Huerta-Cepas, Jaime, Kristoffer Forslund, Luis Pedro Coelho, Damian Szklarczyk, Lars Juhl
521 Jensen, Christian von Mering, and Peer Bork. 2017. "Fast Genome-Wide Functional
522 Annotation through Orthology Assignment by EggNOG-Mapper." *Molecular Biology and
523 Evolution* 34 (8): 2115–22.

- 524 Huerta-Cepas, Jaime, Damian Szklarczyk, Davide Heller, Ana Hernández-Plaza, Sofia K. Forslund,
525 Helen Cook, Daniel R. Mende, et al. 2019. "EggNOG 5.0: A Hierarchical, Functionally and
526 Phylogenetically Annotated Orthology Resource Based on 5090 Organisms and 2502
527 Viruses." *Nucleic Acids Research* 47 (D1): D309–14.
- 528 Imai, B. Y. H. T., C. Baroni Urbani, M. Kubota, G. P. Sharma, M. N. Narasimhanna, B. C. Das, A.
529 K. Sharma, et al. 1984. "Karyological Survey of Indian Ants." *The Japanese Journal of*
530 *Genetics*. <https://doi.org/10.1266/jjg.59.1>.
- 531 Katoh, Kazutaka, and Daron M. Standley. 2013. "MAFFT Multiple Sequence Alignment Software
532 Version 7: Improvements in Performance and Usability." *Molecular Biology and Evolution* 30
533 (4): 772–80.
- 534 Keightley, Peter D., Rob W. Ness, Daniel L. Halligan, and Penelope R. Haddrill. 2014. "Estimation
535 of the Spontaneous Mutation Rate per Nucleotide Site in a *Drosophila Melanogaster* Full-
536 Sib Family." *Genetics* 196 (1): 313–20.
- 537 Keightley, Peter D., Ana Pinharanda, Rob W. Ness, Fraser Simpson, Kanchon K. Dasmahapatra,
538 James Mallet, John W. Davey, and Chris D. Jiggins. 2015. "Estimation of the Spontaneous
539 Mutation Rate in *Heliconius Melpomene*." *Molecular Biology and Evolution* 32 (1): 239–43.
- 540 Kolmogorov, Mikhail, Jeffrey Yuan, Yu Lin, and Pavel A. Pevzner. 2019. "Assembly of Long, Error-
541 Prone Reads Using Repeat Graphs." *Nature Biotechnology* 37 (5): 540–46.
- 542 Konorov, Evgenii A., Mikhail A. Nikitin, Kirill V. Mikhailov, Sergey N. Lysenkov, Mikhail Belenky,
543 Peter L. Chang, Sergey V. Nuzhdin, and Victoria A. Scobeyeva. 2017. "Genomic Exaptation
544 Enables *Lasius Niger* Adaptation to Urban Environments." *BMC Evolutionary Biology* 17
545 (Suppl 1): 39.
- 546 Kuhn, Alexandre, Hugo Darras, Omid Paknia, and Serge Aron. 2020. "Repeated Evolution of Queen
547 Parthenogenesis and Social Hybridogenesis in *Cataglyphis* Desert Ants." *Molecular Ecology*
548 29 (3): 549–64.
- 549 Leniaud, Laurianne, Hugo Darras, Raphael Boulay, and Serge Aron. 2012. "Social Hybridogenesis
550 in the Clonal Ant *Cataglyphis Hispanica*." *Current Biology: CB* 22 (13): 1188–93.

- 551 Lenoir, A., E. Nowbahari, L. Querard, N. Pondicq, and C. Delalande. 1990. "Habitat Exploitation and
552 Intercolonial Relationships in the Ant *Cataglyphis Cursor* (Hymenoptera: Formicidae)." *Acta*
553 *Oecologica* 11 (1): 3–18.
- 554 Li, Heng, and Richard Durbin. 2009. "Fast and Accurate Short Read Alignment with Burrows-
555 Wheeler Transform." *Bioinformatics* 25 (14): 1754–60.
- 556 Li, Heng, Bob Handsaker, Alec Wysoker, Tim Fennell, Jue Ruan, Nils Homer, Gabor Marth, Goncalo
557 Abecasis, and Richard Durbin. 2009. "The Sequence Alignment/Map Format and SAMtools."
558 *Bioinformatics* 25 (16): 2078–79.
- 559 Lieberman-Aiden, Erez, Nynke L. van Berkum, Louise Williams, Maxim Imakaev, Tobias Ragozy,
560 Agnes Telling, Ido Amit, et al. 2009. "Comprehensive Mapping of Long-Range Interactions
561 Reveals Folding Principles of the Human Genome." *Science (New York, N.Y.)* 326 (5950):
562 289–93.
- 563 Liu, Haoxuan, Yanxiao Jia, Xiaoguang Sun, Dacheng Tian, Laurence D. Hurst, and Sihai Yang.
564 2017. "Direct Determination of the Mutation Rate in the Bumblebee Reveals Evidence for
565 Weak Recombination-Associated Mutation and an Approximate Rate Constancy in Insects."
566 *Molecular Biology and Evolution*. <https://doi.org/10.1093/molbev/msw226>.
- 567 Lorite, P., E. Chica, and T. Palomeque. 1996. "Cytogenetic Studies of Ant *Linepithema Humile*
568 *Shattuck* (= *Iridomyrmex Humilis* Mayr) in European Populations." *Caryologia* 49 (2): 199–
569 205.
- 570 Lorite, Pedro, and Teresa Palomeque. 2010. "Karyotype Evolution in Ants (Hymenoptera:
571 Formicidae), with a Review of the Known Ant Chromosome Numbers." *Myrmecological*
572 *News / Osterreichische Gesellschaft Fur Entomofaunistik* 13 (1): 89–102.
- 573 Manni, Mosè, Matthew R. Berkeley, Mathieu Seppey, Felipe A. Simão, and Evgeny M. Zdobnov.
574 2021. "BUSCO Update: Novel and Streamlined Workflows along with Broader and Deeper
575 Phylogenetic Coverage for Scoring of Eukaryotic, Prokaryotic, and Viral Genomes."
576 *Molecular Biology and Evolution* 38 (10): 4647–54.

- 577 Mapleson, Daniel, Gonzalo Garcia Accinelli, George Kettleborough, Jonathan Wright, and Bernardo
578 J. Clavijo. 2016. "KAT: A K-Mer Analysis Toolkit to Quality Control NGS Datasets and
579 Genome Assemblies." *Bioinformatics*, October, btw663.
- 580 Marie-Nelly, Hervé, Martial Marbouty, Axel Cournac, Jean-François Flot, Gianni Liti, Dante Poggi
581 Parodi, Sylvie Syan, et al. 2014. "High-Quality Genome (Re)Assembly Using Chromosomal
582 Contact Data." *Nature Communications* 5 (December): 5695.
- 583 Martin, Marcel. 2011. "Cutadapt Removes Adapter Sequences from High-Throughput Sequencing
584 Reads." *EMBnet.Journal* 17 (1): 10–12.
- 585 Nguyen, Lam-Tung, Heiko A. Schmidt, Arndt von Haeseler, and Bui Quang Minh. 2015. "IQ-TREE:
586 A Fast and Effective Stochastic Algorithm for Estimating Maximum-Likelihood Phylogenies."
587 *Molecular Biology and Evolution* 32 (1): 268–74.
- 588 Obbard, Darren J., John Maclennan, Kang-Wook Kim, Andrew Rambaut, Patrick M. O'Grady, and
589 Francis M. Jiggins. 2012. "Estimating Divergence Dates and Substitution Rates in the
590 *Drosophila* Phylogeny." *Molecular Biology and Evolution* 29 (11): 3459–73.
- 591 Oppold, Ann-Marie, and Markus Pfenninger. 2017. "Direct Estimation of the Spontaneous Mutation
592 Rate by Short-Term Mutation Accumulation Lines in *Chironomus Riparius*." *Evolution Letters*
593 1 (2): 86–92.
- 594 Percy, O. J. Hardy, and S. Aron. 2011. "Automictic Parthenogenesis and Rate of Transition to
595 Homozygosity." *Heredity* 107 (2): 187–88.
- 596 Percy, Morgan, Serge Aron, Claudie Doums, and Laurent Keller. 2004. "Conditional Use of Sex
597 and Parthenogenesis for Worker and Queen Production in Ants." *Science* 306 (5702): 1780–
598 83.
- 599 Peeters, Christian, and Serge Aron. 2017. "Evolutionary Reduction of Female Dispersal in
600 *Cataglyphis* Desert Ants." *Biological Journal of the Linnean Society. Linnean Society of*
601 *London* 122 (1): 58–70.

- 602 Perez, Rémy, and Serge Aron. 2020. "Adaptations to Thermal Stress in Social Insects: Recent
603 Advances and Future Directions." *Biological Reviews of the Cambridge Philosophical*
604 *Society* 95 (6): 1535–53.
- 605 Perez, Rémy, Natalia de Souza Araujo, Matthieu Defrance, and Serge Aron. 2021. "Molecular
606 Adaptations to Heat Stress in the Thermophilic Ant Genus *Cataglyphis*." *Molecular Ecology*
607 30 (21): 5503–16.
- 608 Pfeiffer, Sarah Elisabeth, Verena Luisa Wahl, Matthias Wittlinger, and Harald Wolf. 2019. "High-
609 Speed Locomotion in the Saharan Silver Ant,." *The Journal of Experimental Biology* 222 (Pt
610 20). <https://doi.org/10.1242/jeb.198705>.
- 611 Quesneville, Hadi, Casey M. Bergman, Olivier Andrieu, Delphine Autard, Danielle Nouaud, Michael
612 Ashburner, and Dominique Anxolabehere. 2005. "Combined Evidence Annotation of
613 Transposable Elements in Genome Sequences." *PLoS Computational Biology* 1 (2): 166–
614 75.
- 615 Sanderson, Michael J. 2003. "R8s: Inferring Absolute Rates of Molecular Evolution and Divergence
616 Times in the Absence of a Molecular Clock." *Bioinformatics* 19 (2): 301–2.
- 617 Schrader, Lukas, Jay W. Kim, Daniel Ence, Aleksey Zimin, Antonia Klein, Katharina Wyschetzki,
618 Tobias Weichselgartner, et al. 2014. "Transposable Element Islands Facilitate Adaptation to
619 Novel Environments in an Invasive Species." *Nature Communications*.
620 <https://doi.org/10.1038/ncomms6495>.
- 621 Schwander, Tanja, Laurent Keller, and Sara Helms Cahan. 2007. "Two Alternate Mechanisms
622 Contribute to the Persistence of Interdependent Lineages in Pogonomyrmex Harvester
623 Ants." *Molecular Ecology* 16 (17): 3533–43.
- 624 Simão, Felipe A., Robert M. Waterhouse, Panagiotis Ioannidis, Evgenia V. Kriventseva, and Evgeny
625 M. Zdobnov. 2015. "BUSCO: Assessing Genome Assembly and Annotation Completeness
626 with Single-Copy Orthologs." *Bioinformatics* 31 (19): 3210–12.
- 627 Sommer, Stefan, and Rüdiger Wehner. 2012. "Leg Allometry in Ants: Extreme Long-Leggedness in
628 Thermophilic Species." *Arthropod Structure & Development* 41 (1): 71–77.

- 629 Waterhouse, Robert M., Mathieu Seppey, Felipe A. Simão, Mosè Manni, Panagiotis Ioannidis,
630 Guennadi Klioutchnikov, Evgenia V. Kriventseva, and Evgeny M. Zdobnov. 2017. "BUSCO
631 Applications from Quality Assessments to Gene Prediction and Phylogenomics." *Molecular*
632 *Biology and Evolution*, December. <https://doi.org/10.1093/molbev/msx319>.
- 633 Wehner, R., A. C. Marsh, and S. Wehner. 1992. "Desert Ants on a Thermal Tightrope." *Nature* 357
634 (6379): 586–87.
- 635 Willot, Quentin, Cyril Gueydan, and Serge Aron. 2017. "Proteome Stability, Heat Hardening and
636 Heat-Shock Protein Expression Profiles in Desert Ants." *The Journal of Experimental*
637 *Biology* 220 (Pt 9): 1721–28.
- 638 Xu, Mengyang, Lidong Guo, Shengqiang Gu, Ou Wang, Rui Zhang, Guangyi Fan, Xun Xu, Li Deng,
639 and Xin Liu. 2019. "TGS-GapCloser: Fast and Accurately Passing through the Bermuda in
640 Large Genome Using Error-Prone Third-Generation Long Reads." *BioRxiv*. bioRxiv.
641 <https://doi.org/10.1101/831248>.
- 642 Yahav, Tal, and Eyal Privman. 2019. "A Comparative Analysis of Methods for de Novo Assembly of
643 Hymenopteran Genomes Using Either Haploid or Diploid Samples." *Scientific Reports* 9 (1).
644 <https://doi.org/10.1038/s41598-019-42795-6>.
- 645 Yang, Sihai, Long Wang, Ju Huang, Xiaohui Zhang, Yang Yuan, Jian-Qun Chen, Laurence D. Hurst,
646 and Dacheng Tian. 2015. "Parent-Progeny Sequencing Indicates Higher Mutation Rates in
647 Heterozygotes." *Nature* 523 (7561): 463–67.